Available online at www.sciencedirect.com
SCIENCE DIRECT®
Journal of Nuclear Materials 323 (2003) 304–312
journal of nuclear materials
www.elsevier.com/locate/jnucmat

Brittle fracture and the brittle-to-ductile transition of tungsten

Peter Gumbsch *

Fraunhofer-Institut für Werkstoffmechanik, Wöhlerstraße 11, 79108 Freiburg, Germany
Institut für Zuverlässigkeit von Bauteilen und Systemen, Universität Karlsruhe, Kaiserstraße 12, 76131 Karlsruhe, Germany

Abstract

The aim of this paper is to shortly review the experimental observations and the theoretical understanding of the fracture behaviour of tungsten in the brittle and semi-brittle regime. Advances in the understanding of the mechanisms of fracture processes are made by direct comparison of microscopic modelling and carefully designed experiments. While atomistic simulations are needed to analyse the brittle fracture regime, dislocation simulations are helpful in analysing the dependence of the intrinsic fracture toughness on pre-deformation, temperature or loading rate in the semi-brittle regime below the brittle-to-ductile transition (BDT). By such comparison of fracture experiments on tungsten single crystals with simulations it is shown that dislocation nucleation is the limiting factor at low temperatures, while the dependence on loading rate at intermediate temperatures requires that dislocation mobility takes control. Furthermore, it is shown that the intermediate temperature regime up to the BDT temperature scales with one unique activation energy. At last the results are compared to selected data on polycrystalline tungsten.
© 2003 Elsevier B.V. All rights reserved.

PACS: 62.20.Mk; 61.72.Lk

1. Introduction

The fracture behavior of single and polycrystalline tungsten is characterized by a pronounced brittle-to-ductile transition (BDT) [1–4]. In the low temperature regime, single crystals show cleavage mostly on the low index {1 0 0} and sometimes on the {1 1 0} planes [5]. At intermediate temperatures fracture toughness increases with increasing temperature or decreasing loading rate due to increasing plastic deformation near the crack tip [2]. Theoretical understanding of fracture processes is still rather poor because fracture is a phenomenon which spans many different length scales. The geometry of the specimen and its macroscopic dimensions determine the strength of the stress concentration at the crack tip and are equally important as the microstructure of the material which provides preferred fracture paths. Even the atomic length scale is obviously of importance in the case of brittle fracture, since the crack in a perfectly brittle material moves by breaking individual atomic bonds and must be atomically sharp at its tip. In the semi-brittle regime, the intrinsic brittleness is covered by blunting and shielding of the crack. The fracture toughness of semi-brittle materials as well as the BDT temperature are determined by the competition between the bond-breaking at the crack tip and the mechanisms that govern the crack tip plasticity. A detailed understanding of both of these processes is therefore required to better control materials response with respect to the BDT.

The following chapters will address the questions:

(1) Why is the {1 0 0} plane the preferred cleavage plane of tungsten single crystals?
(2) What are the processes limiting fracture toughness in the semi-brittle regime?
(3) Is fracture toughness linked with the temperature dependence of the flow stress or does it obey another scaling behavior?

* Address: Fraunhofer-Institut für Werkstoffmechanik, Wöhlerstraße 11, 79108 Freiburg, Germany. Tel.: +49-761 52 42 100/721 608 43 63; fax: +49-761 51 42 400/721 608 43 64.
E-mail addresses: gumbsch@iwm.fraunhofer.de, peter.gumbsch@mach.uni-karlsruhe.de (P. Gumbsch).

0022-3115/$ - see front matter © 2003 Elsevier B.V. All rights reserved.
doi:10.1016/j.jnucmat.2003.08.009

(4) Can this information gathered on single crystals be transferred to polycrystalline tungsten?

2. Preferred cleavage planes of tungsten single crystals

Cleavage fracture of elastically (almost) isotropic tungsten single crystals has already been studied quite extensively [2,5–9]. Like other bcc-metals, tungsten primarily cleaves on the $\{1\,0\,0\}$ cleavage plane at room temperature and below [5,9]. On this plane cracks propagate easily in $\langle 0\,1\,1\rangle$ direction, i.e., with a $\langle 0\,1\,\bar{1}\rangle$ crack front. This is seen from the direction of the river lines as well as from the somewhat lower fracture toughness of the $\{1\,0\,0\}$ $\langle 0\,1\,1\rangle$ crack system (crack plane, crack front direction) as compared to the $\{1\,0\,0\}$ $\langle 0\,1\,0\rangle$ crack system [9] (see Table 1).

The secondary cleavage plane, the $\{1\,1\,0\}$ plane, shows an even more pronounced anisotropy. Again the crack with a $\langle\bar{1}\,1\,0\rangle$ crack front has a significantly lower fracture toughness than a crack with a $\langle 0\,0\,1\rangle$ crack front [9]. These two crack planes appear to be the only true cleavage planes of tungsten, although occasionally there are reports of somewhat imperfect $\{2\,1\,1\}$ cleavage facets [8].

Table 1 shows the measured fracture toughness for all four low index cleavage systems at room temperature and below. While the fracture toughness at liquid nitrogen temperature is similar in magnitude for both cleavage planes, the $\{1\,1\,0\}$ cracks show much higher toughness at room temperature. Closer investigation also displays several $\{1\,0\,0\}$ cleavage facets in the fracture surfaces of the room temperature $\{1\,1\,0\}$ specimens [9].

Confronted with the question to predict the favorable cleavage planes of tungsten, one first resorts to the treatment of Griffith, which states that the crack driving force must be larger than the material resistance against fracture. The crack driving force is identified with the energy release rate G and can be obtained from elasticity theory [10].

Accordingly, surfaces with the lowest surface energies should appear as favored cleavage planes. The predominant occurrence of $\{1\,0\,0\}$ cleavage in tungsten can certainly not be explained on this basis, because the close packed $\{1\,1\,0\}$ plane has a markedly lower surface energy than $\{1\,0\,0\}$ and $\{2\,1\,1\}$ planes [11]. Since the Griffith criterion can only be regarded as a necessary condition and not as a fracture criterion it is certainly useful to investigate the atomic bond breaking process in more detail.

Before doing so, it is worth mentioning that previously the plastic relaxation around differently oriented crack tips was held responsible for the preference of the cleavage plane [12]. Specifically for the bcc-transition metals, $\{1\,0\,0\}$ planes should be favored as cleavage plane over $\{1\,1\,0\}$ planes because of the less favorably oriented glide systems. Qualitatively, this point of view would seem to be supported by the room temperature data as shown in Table 1. However, the temperature dependence of the fracture toughness clearly shows, that this argument cannot hold at 77 K. The level of fracture toughness is similar on both planes for cracks with a crack front along the $\langle 1\,1\,0\rangle$ direction.

From an atomistic point of view, one identifies the materials resistance against fracture with the forces needed to break the crack tip bonds successively. In the simplest continuum analogy for the bond breaking, the increase in total surface energy Γ for crack extension from one bond to the next would not be characterized by a linear increase, as assumed in the Griffith criterion, but by a stepwise increase upon breaking of the bond. Such a stepwise increase immediately leads to a finite range of loads, and correspondingly a finite range of stress intensity factors for which the crack remains stable and does not move [13]. Atomistic studies of fracture [14,15] showed that the discrete bond breaking event does indeed manifest itself in such a finite stability range called lattice trapping.

This lattice trapping has been predicted to lead to an anisotropy with respect to the crack propagation direction [15]. Such an anisotropy is now well established for silicon [16] but also occurs in tungsten. The data calculated atomistically for the lattice trapping anisotropy [15] on the basis of the Finnis–Sinclair potential for tungsten [17] are included in Table 1.

Table 1
Fracture toughness of pre-cracked tungsten single crystals for the $\{1\,0\,0\}$ and $\{1\,1\,0\}$ cleavage planes with different crack front directions

Crack system	RT experiments	77 K experiments	Atomistic modeling	BDTT
$\{1\,0\,0\}$ $\langle 0\,1\,0\rangle$	8.7 ± 2.5	3.4 ± 0.6	2.05	470
$\{1\,0\,0\}$ $\langle 0\,1\,1\rangle$	6.2 ± 1.7	2.4 ± 0.4	1.63	370
$\{1\,1\,0\}$ $\langle 0\,0\,1\rangle$	20.2 ± 5.5	3.8 ± 0.4	2.17	430
$\{1\,1\,0\}$ $\langle 1\bar{1}\,0\rangle$	12.9 ± 2.1	2.8 ± 0.2	1.56	370

Data at room temperature and at liquid nitrogen temperature are mean values and standard deviations from at least five individual measurements at almost constant loading rate of 0.10 ± 0.02 MPa $m^{1/2}$ s^{-1}. Atomistic modeling results are from [9]; BDT temperatures are from [2]; fracture toughness is given in MPa $m^{1/2}$.

It remains to ask how an anisotropy in lattice trapping actually can bias one cleavage plane over the other. At first, one could expect both planes to be similarly suitable as cleavage planes because both have one easy crack propagation direction. However, there is an important difference between the two cleavage planes in the number and orientation of the easy propagation directions. The availability of four orthogonal easy directions on the $\{1\,0\,0\}$ crack plane is probably the major cause for its predominance as a cleavage plane. An arbitrarily oriented crack front will always find a vehicle of one or two easy propagation directions and will always exert a significant driving force along the easy directions. In contrast, an arbitrarily oriented crack front on the $\{1\,1\,0\}$ plane will encounter only one easy propagation direction and it will not be able in general to follow it for more than a short distance until it is elongated along a crack front perpendicular to a tough propagation direction which requires a significantly higher driving force.

3. Semi-brittle fracture and the BDT

Crack tip plasticity, essential for semi-brittle fracture and the BDT in tungsten, comprises two distinct processes, nucleation of dislocations at or near the crack tip and the propagation away from the crack. Several models for the BDT describe it as a nucleation-controlled event [18,19], and others focus on dislocation mobility as the controlling factor [20–22]. The temperature at which the BDT occurs [BDT temperature (BDTT)] is strongly dependent on the strain rate, which allows an activation energy for the BDT to be determined. For various other materials this activation energy has been shown to be equal to that for dislocation motion [20,21,23], which suggests a mobility-controlled BDT. On the other hand, specimen size and the availability of dislocation sources have a pronounced influence on the fracture toughness to the degree that they may even switch the material's behavior from brittle to ductile [24], which supports a nucleation-controlled interpretation.

Tungsten single crystal fracture experiments have been performed to determine the characteristics of the fracture toughness below the BDTT and the controlling factors of the BDT [2]. Fracture toughness tests were performed on pre-cracked specimen of four low-index crack systems (Fig. 1). The temperature range covered by the experiments was between liquid nitrogen temperature (77 K) and 650 K. The tests were performed with a constant loading rate. With small variation in the length of the pre-crack this translates into an almost constant stress intensity rate of 0.10 ± 0.02 MPa $m^{1/2}$ s^{-1}. More details of the experimental procedure are given in [25]. Macroscopically, the transition from brittle to ductile response usually correlates with the maximum in fracture toughness. The temperature at this maximum was taken as the BDTT and was determined within 30–60 K (Table 1). The so-defined BDTTs fell into an interval of 100 K for all four crack systems, even though both $\{1\,1\,0\}$ crack systems had a significantly higher room temperature fracture toughness than the $\{1\,0\,0\}$ systems (Table 1).

In tungsten, dislocations penetrating the fracture surface can be made visible by chemical etching with an aqueous solution of $K_3Fe(CN)_6$ and NaOH [26]. This process is highly anisotropic and gives best results on tungsten $\{1\,0\,0\}$ surfaces, whereas no etch pits are produced on $\{1\,1\,0\}$ surfaces [27]. Dislocation etch pits on the $\{1\,0\,0\}$ $\langle 0\,1\,0\rangle$ fracture surface produced at 77 K reveal the activity of only a few discrete dislocation sources at the arrest line of the pre-crack [2]. In contrast, after fracture at room temperature, dislocation etch pits show a very dense population of dislocation sources along the crack front. The length of the dislocation traces emanating from these sources, however, is only slightly greater than in the low-temperature fracture. A

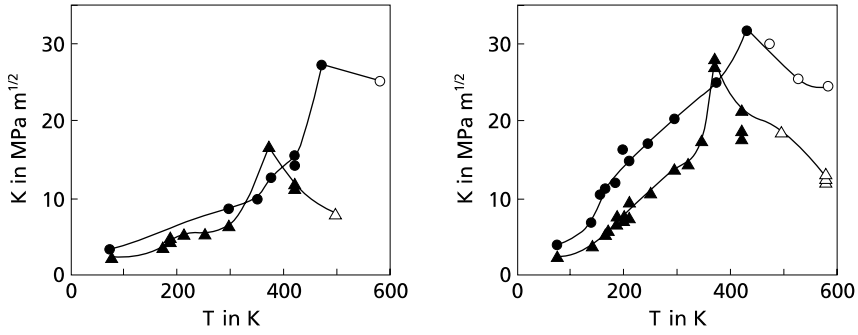

Fig. 1. Temperature dependence of fracture toughness of tungsten single crystals for the four low index crack systems. Results for $\{1\,0\,0\}$ fracture surfaces are displayed in the left frame, and those for $\{1\,1\,0\}$ fracture surfaces are shown in the right frame. The $\langle 0\,0\,1\rangle$ crack front is indicated by circles and the $\langle 0\,1\,1\rangle$ front is indicated by triangles in both cases.

high density of dislocation sources along the crack tip is necessary to produce global shielding of the crack tip, because the zone of effective shielding may be localized around a source [28]. Only when this global shielding is achieved does the size of the plastic zone, and thus dislocation mobility, become important.

Evidence for the importance of the number of active dislocation sources can be obtained from experiments on pre-deformed samples where the pre-existing dislocation density and the availability of dislocation sources is increased before toughness testing. Specimens with a $\{1\,0\,0\}\ \langle 0\,1\,0\rangle$ crack system were deformed by compression along the $\langle 1\,1\,0\rangle$ axis at 400 °C to a plastic strain of $\varepsilon_{pl} = 0.1$ before pre-cracking. At low temperatures the pre-deformed specimens are significantly tougher than the undeformed specimens (Fig. 2). However, their fracture toughness remains almost constant, increasing only marginally up to 370 K. Above this temperature a drastic increase in fracture toughness is observed. The BDT occurs at about 470 K, which is 100 K higher than in the undeformed material. The only reasonable explanation for the increase of low temperature fracture toughness with pre-deformation is that pre-existing dislocations in the highly stressed vicinity of the crack tip act as sources for dislocations, which provide more efficient shielding.

At intermediate temperatures, the beneficial effect of the pre-deformation vanishes and the fracture toughness of the pre-deformed specimens is lower than that of the reference specimens. This is attributed to the increased yield strength and lower dislocation mobility produced by work hardening. The reduced dislocation mobility will not only decrease the fracture toughness but must also be expected to shift the BDTT to higher temperatures. These observations strongly indicate that the BDT is controlled by dislocation mobility.

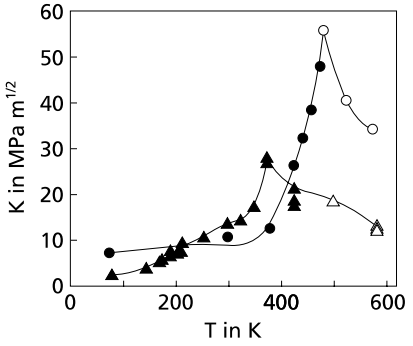

Fig. 2. Temperature dependence of fracture toughness for pre-deformed samples (circles) compared with undeformed reference samples (triangles). Filled symbols give stress intensity factors; open symbols are maximum stresses at failure for ductile behavior (normalised by the crack length).

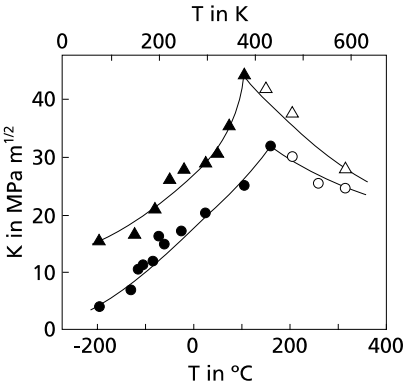

Fig. 3. Fracture toughness measured on tungsten samples with $(0\,1\,1)\ [1\,0\,0]$ crack system in pre-cracked (circles) and notched (triangles) specimens.

At low temperatures, dislocation nucleation is the limiting process because of the scarcity of active sources. When the temperature is sufficiently high to activate a large number of sources or if the number of active sources is increased by pre-deformation, dislocation mobility assumes control of the nucleation rate, and the fracture toughness becomes rate dependent. The loading rate dependence of the fracture toughness of tungsten can be interpreted in terms of dislocation processes and is discussed in the next chapter. However, detailed quantitative understanding of the fracture toughness itself and its dependence on the crystallographic orientation of the cleavage system is still lacking.

Fracture toughness of tungsten single crystals so far was only reported here for specimens with sharp pre-cracks induced at liquid nitrogen temperature using a sophisticated bridge technique [25]. Fracture toughness determined in this way is significantly lower than toughness determined from fatigue pre-cracks or sawn notches. As an example, the temperature dependence and the BDT of the $\{0\,1\,1\}\ \langle 1\,0\,0\rangle$ crack systems in tungsten is shown in Fig. 3 both for a sharp pre-crack and a sawn notch with a radius of curvature at the tip of approximately 100 μm. Compared to the sharp cracks, the blunt notch results in a higher apparent fracture toughness at low temperature because the stress concentration at the crack tip is less pronounced. It also results in a decrease of the BDT temperature. This decrease is of course even more pronounced in unnotched specimens which can be deformed in tension down to liquid helium temperature without fracturing [29].

4. Strain rate dependence

Both the BDTT and the fracture toughness in the semi-brittle regime exhibit a pronounced dependence on loading rate. At constant temperature, polycrystalline

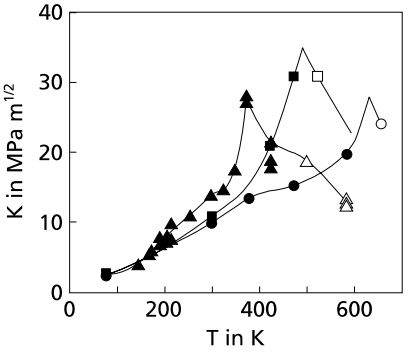

Fig. 4. Fracture toughness K_{crit} of pre-cracked tungsten single crystals as a function of temperature T for different loading rates $\dot{K}$ (MPa m$^{1/2}$ s^{-1}). Filled symbols give stress intensity factors; open symbols are maximum stresses at failure for ductile behaviour (normalised by the crack length). The crack system specified by the nominal crack plane and the crack front direction was $\{1\,1\,0\}\ \langle 1\bar{1}0\rangle$. (Triangles, $\dot{K} = 0.1$ MPa m$^{1/2}$ s^{-1}; squares, $\dot{K} = 0.4$ MPa m$^{1/2}$ s^{-1}; circles, $\dot{K} = 1.0$ MPa m$^{1/2}$ s^{-1}). Data taken from Ref. [2].

tungsten can change from brittle fracture to ductile response as the shear rate is decreased [30,31]. Correspondingly the BDTT has been found to increase for increasing strain rate [32]. Probably the most detailed information on the loading rate dependence is available for $\{1\,1\,0\}$ cracks in tungsten single crystals with nominal $\langle 1\bar{1}0\rangle$ crack fronts [2]. Except for 77 K, where loading rate does not change the measured fracture toughness, a higher loading rate always lowers the fracture toughness (Fig. 4) at higher temperatures. At room temperature, the fracture toughness decreases linearly with the logarithm of the loading rate from 16 to 6 MPa m$^{1/2}$ when the loading rate is increased from 0.04 to 6 MPa m$^{1/2}$ s^{-1}. Furthermore, the BDTT occurs at similar stress levels and increases significantly with the loading rate. In an Arrhenius plot ($\log \dot{K}$ versus 1/BDTT), all values fall on a straight line, yielding an activation energy for the BDT in tungsten of $Q_{BDT} \approx 0.2$ eV.

Discrete dislocation dynamics simulation of crack tip plasticity [33,34] have shown that the dependence on loading rate can directly be linked to the strain rate dependence of the plastic relaxation around the crack tip. Using the Orowan law

$$\dot{\varepsilon}(\tau, T) = b\rho V_d(\tau, T), \tag{1}$$

the plastic relaxation rate $\dot{\varepsilon}$ is directly connected with the velocity law of the dislocations via the dislocation density ρ and the Burgers vector b. In the simplest and most approximate form, the mobility of the dislocations is described by an Arrhenius type law of the form [35,36]

$$V_d(\tau, T) = A\left(\frac{\tau}{\tau_0}\right)^m \exp\left(-\frac{Q_d}{k_B T}\right), \tag{2}$$

where the dislocation velocity V_d depends on the resolved shear stress τ, the stress exponent m, the temperature T and the activation energy Q_d. The parameter A is a pre-exponential factor with the units of a velocity; $\tau_0 = 1$ MPa simply fixes the units of the stress. The Boltzmann constant is denoted with k_B.

The strain rate and temperature dependence of the fracture toughness that is obtained from the numerical simulations reflects all the non-linearities of the thermally activated motion of many dislocations in the field of the crack. However, simulations in which an equal number of dislocations is emitted show practically the same fracture toughness, just like the experimentally determined fracture toughness always assumes a similar value at the BDTT. This means that loading rate and temperature are strongly correlated at points of constant fracture toughness and obey a scaling relation which leads to one unique master curve for the temperature dependence of the fracture toughness.

An implicit formulation of this scaling relation between the loading rates $\dot{K}_i$ and the temperatures T_i, at which a given fracture toughness K_{crit} is reached, reads:

$$K_{crit}(\dot{K}_i, T_i) = \text{constant}. \tag{3}$$

It is evident that this equation cannot be fulfilled for every K_{crit} in the set of results if $\dot{K}_i$ and T_i are unrelated. The relation between these two quantities is the desired scaling relation, for which a simple Arrhenius ansatz gives:

$$\boldsymbol{T_2} = \left[\frac{k_B}{U_{scaling}} \ln\frac{\dot{K}_1}{\dot{K}_2} + \frac{1}{T_1}\right]^{-1}, \tag{4}$$

where $U_{scaling}$ is the activation energy of the relevant process.

Provided this scaling law is valid, every T–K_{crit} curve obtained for the loading rate $\dot{K}_1$ can be transformed into a T–K_{crit} curve for the loading rate $\dot{K}_2$ through an appropriate scaling of the temperature axis. This scaling behavior can thus be used to obtain a value for the apparent activation energy for the crack tip plasticity. Fig. 5 shows that the experimentally determined fracture toughness of tungsten single crystals displayed in Fig. 4, scales, according to Eq. (2), over the entire temperature range where dislocation motion is assumed to control fracture toughness. The scaling of the experimental data gives an apparent activation energy of $U_{scaling} = 0.19$ eV.

This activation energy is far too low to be reconciled with the activation energy for bulk plasticity. In the entire temperature regime of the present investigation, bulk plasticity in tungsten is believed to be controlled by the mobility of screw dislocations (see, for example [29,37,38]). The activation energy for the glide of these dislocations is $Q_{screw} = 2$ eV [38] and is therefore about one order of magnitude higher than $U_{scaling}$. While a

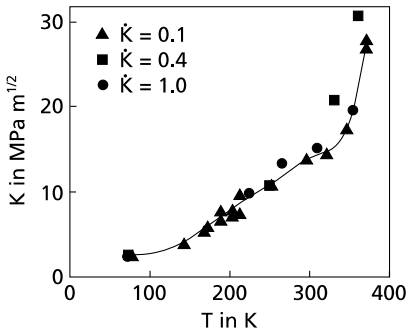

Fig. 5. Experimental data on tungsten single crystals from Fig. 3 in a fracture toughness–temperature plot with rescaled temperature axis. The basis loading rate is $\dot{K}_2 = 0.1$ MPa m$^{1/2}$ s^{-1}; all loading rates given in the key are in units of MPa m$^{1/2}$ s^{-1}. The apparent activation energy of crack-tip plasticity has been determined to be $U_p = 0.19$ eV.

strong stress dependence could decrease the effective Q_{screw} to somewhat lower values, it does not seem plausible that it is decreased by a full order of magnitude and within the entire low temperature regime. Simulations with more sophisticated mobility laws [34] indeed confirm that the effective decrease is by far not large enough to explain this discrepancy. Consequently, it is concluded that crack tip plasticity and bulk deformation cannot be controlled by the same mechanisms. It could now either be argued that crack tip plasticity is entirely dominated by processes at the very tip of the crack, where the stress fields are sufficiently high to effectively reduce the Peierls barrier for the screw dislocations, which also does not appear to be an appealing explanation, or the mobility of non-screw dislocations, but not the mobility of the screw dislocations, is controlling the fracture toughness in the semi-brittle regime blow the BDT. Since the non-screw dislocations provide all the shielding to the crack tip, this observation is certainly worth further investigation. In any case, the details of the crack tip sources and dislocations multiplication processes near the crack tip need to be studied further to answer the question whether they can provide enough non-screw dislocations to produce sufficient shielding and blunting of the crack tip to induce the transition to ductile behavior.

A practical use of the derived scaling relation is that for a given material the fracture toughness in the semi-brittle regime and the BDT can be predicted for different temperatures and loading rates. This requires the knowledge of a fracture toughness–temperature-curve for a single loading rate and the apparent activation energy for crack-tip plasticity, which can be derived from single experiments for at least two different loading rates. Such a model-based extrapolation of experimental data can in principle save quite a large number of experiments and, moreover, the fracture toughness can be predicted for temperatures or loading rates that are not easy to establish in experiments.

It is noted that the model of crack-tip plasticity presented in [33,34] cannot predict the exact shape of the single crystal 'master curve' itself and in particular does not show a transition to purely ductile behavior. This must be attributed to the simplifications of this model. The most severe simplifications in this respect are the neglect of dislocation multiplication and of the blunting of the crack tip. Especially in simulations, where thousands of dislocations are nucleated, the blunting of the crack tip must be taken into account. Since a blunted crack cannot propagate through the crystal, an atomically sharp crack has to be re-initiated to permit crack advance. For a radius of curvature of the blunted crack tip above a few Burgers vectors, the critical stress intensity for re-initiation becomes increasingly more difficult for larger amounts of blunting [39,40]. The blunting of the crack tip is proportional to the number of dislocations and, therefore, it is also rate dependent. Current modelling efforts are directed towards the quantitative determination of the contribution of blunting to fracture toughness, impedes crack advance and how it affects the dislocation nucleation in its vicinity [39,41–43].

5. Fracture of polycrystalline tungsten rods

Polycrystalline tungsten is usually produced by powder metallurgical roots and is commercially available in many forms. It will not be possible to review here all varieties. With the aim of comparing to the single crystal data, the focus is put on just one very common variety, sintered and swaged tungsten rods. Typical for such unrecrystallized swaged, extruded or rolled cylindrical rods made from bcc metals is a fairly strong $\langle 1\,1\,0\rangle$ fibre texture [44] and a grain structure elongated along the axis of the rod. For the swaged tungsten used in [44] the aspect ratio of the grains is about 4:1.

Plasticity and the failure of tungsten rods or wires fabricated from the rods have been studied quite extensively. Data are available for various strain rates [1,3,30–32], different loading nodes [45] and different processing conditions [3,46,47]. Dedicated fracture studies with notched or pre-cracked specimens, however, are scarce. Some fracture data is available on tungsten and tungsten–rhenium alloys [48–52] but specimen conditions and microstructure are not well analyzed. A few detailed fracture experiments on textured polycrystalline rods are available, which allow to make contact to the single crystal experiments [25,44]. These will be discussed in the following.

Two types of bend specimens were taken from the swaged rods [44]. Longitudinal specimens have the long

Table 2
Mode I fracture toughness of polycrystalline and single crystal tungsten fracture toughness (MPa $m^{1/2}$)

Sample	Liquid nitrogen	Room temperature
Longitudinal	11.5 ± 0.3	12.6 ± 1.3
Longitudinal pre-deformed		19.5 ± 0.3
Transverse	5.9 ± 0.3	8.0 ± 0.2
{1 1 0} single crystal	2.8–3.8[a]	12.9–20.2[a]

Data from Ref. [25].
[a] Range of values represents different crack propagation directions.

axis parallel to the swaging direction. Under mode I loading the fracture planes correspond to the {1 1 0} texture planes and are perpendicular to the long axis of the grains. Transverse specimens have their long axis perpendicular to the swaging direction and mode I fracture proceeds along the swaging direction. The measured fracture toughness from pre-cracked specimens is summarized in Table 2.

The results for the longitudinal liquid nitrogen specimen is a statistical average of specimens, one of which did not fracture catastrophically but could be controlled during fracture [25]. At room temperature a value of 12.6 ± 1.3 MPa $m^{1/2}$ was obtained from 13 specimens, all of which fractured catastrophically. Crack propagation for the transverse specimens was always stable and showed significant R curve behaviour. The data included in Table 2 is from the first propagation after pre-cracking. The fracture surfaces of the longitudinal specimens primarily show transcrystalline cleavage but also a smaller amount of intercrystalline fracture which increases from liquid nitrogen temperature to room temperature from below 10% of the fracture surface area to about a third. Side cracks along grain boundaries perpendicular to the main propagation direction are observed at the location of the stopped precrack or after longer jumps of the crack. The fracture surfaces of the transverse specimens show mainly intergranular fracture both at liquid nitrogen temperature and at room temperature.

Mixed mode I/II experiments conducted on longitudinal specimens at room temperature [44] give results between the longitudinal and the transverse specimens both in the appearance of the fracture surfaces and in measured fracture toughness.

One of the longitudinal specimens was deformed in cyclic compression at room temperature before precracking at 77 K and toughness testing at room temperature [25]. This specimen gave controlled crack growth at a significantly higher fracture toughness than the undeformed specimens. Nevertheless, the fracture surface was almost entirely transgranular with the exception of a few 'holes' where apparently a few entire grains had been pulled out of the fracture surface.

Because the polycrystalline material shows a {1 1 0} fiber texture along the axis of the specimen, transgranular fracture in the longitudinal samples generally occurs on {1 1 0} cleavage planes. The weak temperature dependence of the fracture toughness of the polycrystalline material studied here is, at first, difficult to understand if it is compared to the results for the {1 1 0} cleavage fracture toughness of tungsten single crystals [2,9]. The {1 1 0} fracture toughness of the single crystals rises significantly from 2.8 to 3.8 MPa $m^{1/2}$ at liquid nitrogen temperature to 12.0 to 20.2 MPa $m^{1/2}$ at room temperature (see Table 2). The polycrystals give an almost constant fracture toughness which is somewhat lower than for the single crystals at room temperature but three times higher at liquid nitrogen temperature.

At liquid nitrogen temperature, it could be suggested that if the energy supplied to the system is going to cleave {1 1 0} planes only, to a first approximation it should not matter whether it were a single crystal or a highly textured polycrystal. The fracture surfaces of the longitudinal specimens loaded in pure mode I showed some intergranular fracture, which is slightly more pronounced at room temperature than at liquid nitrogen temperature. Fracture on grain boundaries parallel to the swaging axis was also observed. It is likely that grain boundary fracture of the polycrystal absorbs a considerable amount of the fracture energy. It therefore seems justified to attribute the higher toughness of the polycrystal as compared to the single crystal at liquid nitrogen temperature to (1) the side branching of cracks onto surfaces along the long axis of the grain structure and (2) of course also the imperfect texture of the polycrystal. For fracture at room temperature these toughness increasing factors do not change much, but the weak boundaries play a somewhat more important role, which is manifest in the higher degree of intercrystalline fracture. The small grain size and the higher dislocation density of the swaged polycrystal as compared to the single crystal in this sense leads to a behaviour which rather compares in the toughness versus temperature behaviour to the pre-deformed single crystal. The pre-deformed single crystal also did not show a significant dependence of fracture toughness on temperature in this temperature regime. Further

pre-deformation further increases fracture toughness. However, it remains unclear whether this is an intrinsic effect of increased dislocation activity as in the single crystals, or an extrinsic effect due to extensive microcrack toughening. Certainly, the observations of the 'holes' on the fracture surface and the somewhat rougher appearance of the fracture surfaces show that some of the additional energy consumption is due to such extrinsic bridging effects. The fracture toughness of the transverse specimens and its weak temperature dependence can certainly be attributed entirely to such extrinsic toughening effects.

6. Summary

The fracture behaviour of tungsten has been very well studied for single crystals. These experiments lend themselves well as model experiments which can directly be interpreted in terms of simple fundamental models. The role of dislocation sources and dislocation mobility as well as the scaling of the fracture toughness with temperature and loading rates can well be interpreted in terms of such simple models.

The understanding of slightly more complicated microstructures and particularly of pre-deformed single crystals and/or textured and possibly pre-deformed polycrystalline materials is far less well understood. Starting from the excellent date base from the single crystals, there is, however, great expectation that more complicated microstructures can be interpreted similarly well. However, significantly more experiments are needed to discriminate there between the role of dislocations, microcracking, branching of the main crack and crack bridging effects.

References

[1] H. Lassila, G.T. Gray, J. Phys. IV Colloque C8 4 (supplément au Journal de Physique III) (1994) C8-349.
[2] P. Gumbsch, J. Riedle, A. Hartmaier, H.F. Fischmeister, Science 282 (1998) 1293.
[3] T. Dümmer, J.C. Lasalvia, G. Ravichandran, M.A. Meyers, Acta Mater. 46 (1998) 6267.
[4] S.J. Zinkle, N.M. Ghoniem, Fusion Eng. Design 51–52 (2000) 55.
[5] D. Hull, P. Beardmore, A.P. Valentine, Philos. Mag. 12 (1965) 1021.
[6] J.E. Cordwell, D. Hull, Philos. Mag. 26 (1972) 215.
[7] J.M. Liu, J.C. Bilello, Philos. Mag. 35 (1977) 1453.
[8] J. Riedle, P. Gumbsch, H.F. Fischmeister, V.G. Glebovsky, V.N. Semenov, Mater. Lett. 20 (1994) 311.
[9] J. Riedle, P. Gumbsch, H.F. Fischmeister, Phys. Rev. Lett. 76 (1996) 3594.
[10] R. Thomson, Solid State Phys. 39 (1986) 1.
[11] M. Methfessel, D. Hennig, M. Scheffler, Phys. Rev. B. 46 (1992) 4816.
[12] R.A. Ayres, D.F. Stein, Acta Metall. 19 (1971) 789.
[13] P. Gumbsch, R.M. Cannon, MRS Bull. 25/5 (2000) 15.
[14] R. Thomson, C. Hsieh, V. Rana, J. Appl. Phys. 42 (1971) 3154.
[15] S. Kohlhoff, P. Gumbsch, H.F. Fischmeister, Philos. Mag. A 64 (1991) 851.
[16] R. Pérez, P. Gumbsch, Phys. Rev. Lett. 84 (2000) 5347.
[17] M.W. Finnis, J.E. Sinclair, Philos. Mag. A 50 (1984) 45; with corrections from G.J. Ackland, R. Thetford, Philos. Mag. A 56 (1987) 15.
[18] J.R. Rice, R. Thomson, Philos. Mag. A 29 (1974) 73.
[19] M. Khantha, D. Pope, V. Vitek, Phys. Rev. Lett. 73 (1994) 684.
[20] P.B. Hirsch, S.G. Roberts, J. Samuels, Proc. R. Soc. London, Ser. A 421 (1989) 25.
[21] S.G. Roberts, in: H.O. Kirchner, L.P. Kubin, V. Pontikis (Eds.), Computer Simulations in Materials Science, series E: Applied Sciences, vol. 308, Kluwer, Dordrecht, 1996, p. 409.
[22] A. Hartmaier, P. Gumbsch, Phys. Status Solidi (b) 202 (1997) R1.
[23] M. Brede, P. Haasen, Acta Metall. 36 (1988) 2003-03-17.
[24] G. Michot, M.A.L. de Oliveira, A. George, Mater. Sci. Eng. A 176 (1994) 99.
[25] J. Riedle, thesis, Universität Stuttgart, Stuttgart, 1995.
[26] L. Berlec, J. Appl. Phys. 33 (1962) 197.
[27] Y. Tamura, T. Fujii, Y. Ohba, Trans. Inst. Met. 14 (5) (1972) 173.
[28] B. Devincre, S.G. Roberts, Acta Mater. 44 (1996) 2891.
[29] D. Brunner, Mater. Trans. 41 (2000) 152.
[30] G. Subhash, Y.J. Lee, G. Ravichandran, Acta Metall. 42 (1994) 319.
[31] G. Subhash, Y.J. Lee, G. Ravichandran, Acta Metall. 42 (1994) 331.
[32] A.C. Chilton, A.S. Wronsky, J. Less-common Metals 17 (1969) 447.
[33] A. Hartmaier, P. Gumbsch, J. Computer-Aided Mater. Design 6 (1999) 145.
[34] A. Hartmaier, P. Gumbsch, Philos. Mag. A 82 (2002) 3187.
[35] H.W. Schadler, Acta Metall. 12 (1964) 861.
[36] U.F. Kocks, A.S. Argon, M.F. Ashby, Prog. Mater. Sci. 19 (1975), chapters 3 + 4, p. 68.
[37] A.S. Argon, S.R. Maloof, Acta. Metall. 14 (1966) 1449.
[38] D. Brunner, J. Diehl, V. Glebovsky, in: Proceedings of the Fifth International Conference on Ultra High Purity Materials (UHPM-98), Sevrier, Annecy Lake, France, 1998, p. 83.
[39] P. Gumbsch, J. Mater. Res. 10 (1995) 2897.
[40] G.E. Beltz, D.M. Lipkin, L.L. Fischer, Phys. Rev. Lett. 82 (1999) 4468.
[41] E. Van der Giessen, V.S. Deshpande, H.H.M. Cleveringa, A. Needleman, J. Mech. Phys. Solids 49 (2001) 2133.
[42] H.H.M. Cleveringa, E. Van der Giessen, A. Needleman, J. Mech. Phys. Solids 48 (2000) 1133.
[43] L.L. Fischer, G. Beltz, J. Mech. Phys. Solids 49 (2001) 635.
[44] R.W. Margevicius, J. Riedle, P. Gumbsch, Mater. Sci. Eng. A 270 (1999) 197.
[45] W.-S. Lee, C.-F. Lin, G.-L. Xiea, Mater. Sci. Eng. A 247 (1998) 102.
[46] P.P. Bourque, D.F. Bahr, M.G. Norton, Mater. Sci. Eng. A 298 (2001) 73.

[47] J. Warren, A.D. Jackson, Scr. Mater. 34 (1996) 787.
[48] C.W. Marshall, F.C. Holden, in: R.W. Fountain et al. (Eds.), High Temperature Refractory Metals: Metallurgical Society Conference 34, Gordon and Breach, New York, 1966, p. 129.
[49] A.V. Babak, E.I. Uskov, Strength Mater. 16 (1984) 943.
[50] Y.N. Podrezov, O.G. Radchenko, N.G. Danilenko, V.V. Panichkina, V.I. Gachegov, O.B. Ol'shanskii, Sov. Powder Metall. Metal Ceram. 26 (1987) 677.
[51] Y. Mutoh, K. Ichikawa, K. Nagata, M. Takeuchi, J. Mater. Sci. 30 (1995) 770.
[52] Tran-Huu-Loi, J.P. Morniroli, M. Gantois, M. Lahaye, J. Mater. Sci. 20 (1985) 199.